



Search of the Lightest Scalar Top \tilde{t}_1 in
 $\tilde{t}_1\tilde{t}_1 \longrightarrow b\bar{b} \mu^+\mu^- \tilde{\nu}\tilde{\nu}$
Decays at DØ

The DØ Collaboration
URL <http://www-d0.fnal.gov>
(Dated: July 12, 2005)

We report preliminary results on a search for the lightest supersymmetric partner of the top quark \tilde{t}_1 in final states with two muons, at least one b quark jet and missing transverse energy, using 339 pb^{-1} of data collected by the DØ experiment at Fermilab Tevatron Collider in 2002-2004 (Run II). The data analysis is based on a selection using event topology and presence of at least one b quark jet. We improve existing limits for stop and sneutrino masses in $[90, 120]$ GeV/c^2 and $[70, 85]$ GeV/c^2 mass ranges respectively.

I. INTRODUCTION

Supersymmetric theories (SUSY) [1] predict the existence of a left- and right-handed scalar partner, eigenstates of the SUSY lagrangian, for each standard model fermion. Because of the large mass of the standard model top quark, the mixing between its chiral supersymmetric partners is the largest among all squarks; therefore the lightest supersymmetric partner of the top quark, \tilde{t}_1 , might be the lightest squark, whose discovery would be an opening to the SUSY world.

Recent theoretical studies [2] have shown that the \tilde{t}_1 decays into charm quark and neutralino ($\tilde{\chi}_1^0$), which has been until now the most explored scenario for \tilde{t}_1 searches, might not be the dominant ones for \tilde{t}_1 masses accessible at the Tevatron. Furthermore, these studies favor three-body decays of the \tilde{t}_1 into $bW\tilde{\chi}_1^0$ and/or $bl\tilde{\nu}$ (where $\tilde{\nu}$ is a sneutrino) via a virtual chargino $\tilde{\chi}^\pm$. If the mass of the sneutrino $\tilde{\nu}$ is much greater than the W mass, the $bW\tilde{\chi}_1^0$ decays will dominate; if the mass of the sneutrino is of the same order as the mass of the W, decays to $bl\tilde{\nu}$ will dominate.

Since decays of the \tilde{t}_1 in the W-exchange scenario have very limited discovery potential for the Run II, we will in this analysis focus on the sneutrino-exchange scenario of the \tilde{t}_1 :

$$\tilde{t}_1\bar{\tilde{t}}_1 \rightarrow b\bar{b} \tilde{\chi}^+ \quad \tilde{\chi}^- \\ \hookrightarrow \mu^+\tilde{\nu} \rightarrow \mu^+\nu\tilde{\chi}_1^0 \quad \hookrightarrow \mu^-\tilde{\nu} \rightarrow \mu^-\nu\tilde{\chi}_1^0$$

where a virtual chargino $\tilde{\chi}^\pm$ decays into a muon and a sneutrino $\tilde{\nu}$; the $\tilde{\nu}$ decays into a neutrino and a neutralino $\tilde{\chi}_1^0$, considered to be the Lightest Supersymmetric Particle (LSP). The Minimal Supersymmetric Standard Model (MSSM) is the theoretical framework for this search, where we consider the $\mu^+\mu^- b\bar{b} + \cancel{E}_T$ final state from the \tilde{t}_1 pair production.

II. DATA AND MONTE-CARLO SAMPLE

The data sample consists of the data taken by the DØ detector from 2002 through 2004. The trigger selection requires two muons to be present in the event. After trigger and data quality requirements, the data has an integrated luminosity of 339 pb⁻¹.

For the simulation of the three-body decays of the \tilde{t}_1 , the Monte Carlo generators CompHEP [3] and PYTHIA 6.202 [4] have been successively used for the generation of the particles and the hadronization of the quarks. The different MSSM parameters for various SUSY signal points ($M(\tilde{t}_1), M(\tilde{\nu})$) are displayed on Tab. I. The branching ratio of the lightest chargino $\tilde{\chi}_1^\pm$ decaying into $\tilde{\nu}$'s is assumed to be 100%; slepton parameters, including the trilinear stau mixing term, have been set to obtain equal branching fraction of $\tilde{\chi}_1^\pm$ decaying into all lepton flavors. The parameter values $\tan\beta = 20$, $\mu = +225$ GeV, $M(\tilde{g}) = 500$ GeV/c², $M(H_A) = 800$ GeV/c² are common to all points, while :

- A_T , the trilinear stop mixing term, has been varied to obtain the mass of the \tilde{t}_1 ,
- $M_{L1,2}$, which are the masses of the two first generation left sleptons, have been varied to obtain the masses of electron- and muon- $\tilde{\nu}$,
- M_1 , the bino mass, is used to keep the lightest neutralino $\tilde{\chi}_1^0$ as LSP, and such that $M(\tilde{\nu}) \geq M(\tilde{\chi}_1^0)$,
- M_2 , the wino mass, is used to keep the lightest chargino $\tilde{\chi}^\pm$ virtual.

The choice of an intermediate value of $\tan\beta$ is to favor three-body decays of the \tilde{t}_1 [2]; susy parameters are taken real and CP phases are neglected. In the same table are also shown the total next-to-leading order cross section and the number of generated events. Signal points with a low $\Delta m = M(\tilde{t}_1) - M(\tilde{\nu})$ will be referred as soft signals.

The background samples have been generated using PYTHIA. Channels involving the Z boson, which are the dominant background, have been reweighted as a function of the p_T of the Z to reproduce the experimental differential cross section $d\sigma(Z)/dp_T$. Finally, the multijet background where two muons can be present, i.e. QCD background, also contributes to the selected sample; rather than resort to Monte Carlo simulation, we determine the QCD contribution from the data by considering the ratio of opposite- to like-sign dimuons times like-sign data events surviving muon isolation cuts.

III. PRESELECTION AND DATA/BACKGROUND COMPARISON

In this analysis, we require two opposite charge muons :

- with hits in the inner and outermost wire- and scintillator-layers of the muon detector,

TABLE I: Overview of the different SUSY signal points $(M(\tilde{t}_1), M(\tilde{\nu}))$ as simulated by CompHEP for $\tan\beta = 20$, $\mu = +225$ GeV, $M(\tilde{g}) = 500$ GeV/ c^2 , $M(H_A) = 800$ GeV/ c^2 , and the corresponding MSSM parameters and the total cross section as obtained from PROSPINO [5].

Signal points	A_T [GeV]	$M_{L1,2}$ [GeV/ c^2]	M_1 [GeV/ c^2]	M_2 [GeV/ c^2]	$M(\tilde{t}_1)$ [GeV/ c^2]	$M(\tilde{\nu})$ [GeV/ c^2]	$\sigma \cdot Br$ [pb]
A1	510	82	53.5	215	70.63	50.86	10.83
A2	501.5	82	53.5	215	80.06	50.86	5.56
A3	480	82	53.5	210	100.03	50.86	1.65
A4	453	82	53.5	225	120.50	50.86	0.58
A5	438	82	53.5	225	130.49	50.86	0.37
A6	422.5	82	53.5	230	140.07	50.86	0.25
A7	413	82	53.5	230	145.63	50.86	0.20
A8	405	82	53.5	250	150.16	50.86	0.16
A9	386	82	53.5	275	160.39	50.86	0.11
B1	501.5	88.5	63	215	80.06	60.80	5.56
B2	491.2	88.5	63	215	90.18	60.80	2.92
B3	480	88.5	63	210	100.03	60.80	1.65
B4	453	88.5	63.7	225	120.50	60.80	0.58
B5	422.5	88.5	63.7	230	140.07	60.80	0.25
B6	405	88.5	63.7	250	150.16	60.80	0.16
C1	491.2	95.5	74	215	90.18	70.60	2.92
C2	480	95.5	74	210	100.03	70.60	1.65
C3	467	95.5	74	210	110.36	70.60	0.96
C4	438	95.5	74	225	130.49	70.60	0.37
C5	422.5	95.5	74	230	140.07	70.60	0.25
C6	405	95.5	74	250	150.16	70.60	0.16
D1	480	103	85	210	100.03	80.45	1.65
D2	467	103	85	210	110.36	80.45	0.96
D3	453	103	85	225	120.50	80.45	0.58
D4	438	103	85	225	130.49	80.45	0.37
D5	422.5	103	85	230	140.07	80.45	0.25
D6	405	103	85	250	150.16	80.45	0.16

- matched to a track in the central tracking detector,
- surviving a timing cut suppressing the muons originating from cosmic radiation,
- having at least one hit in the silicon tracker,
- isolated from jet activity :
 - $\sum_i^{tracks} p_T(i) < 4$ GeV/ c , where the sum is over all charged tracks in a cone of $dR = 0.5$ around the muon, except the muon itself,
 - $[E_T^{(R=0.4)} - E_T^{(R=0.1)}] < 4$ GeV/ c , where E_T^R is the transverse energy as measured by the calorimeter in a radius R around the muon.

Since the acceptance of the SMT detector is $|\Delta z| < 35cm$, events are required to have the z of the primary vertex within this limit. In order to further diminish the QCD contribution to the selected sample while retaining soft signals, the highest p_T muon (μ_1) and next to highest p_T muon (μ_2) are required to have p_T greater than 8 and 6 GeV/ c . The missing transverse energy \cancel{E}_T is corrected with the jet energy scale [6].

Since the \cancel{E}_T is a key variable of this analysis, and it is corrected from the momentum of the muons, it is important to ensure the quality of the muons with respect to the \cancel{E}_T . In a dimuon event, significant mismeasurement of muon momenta can lead to strong angular correlation between the muon direction and the \cancel{E}_T direction; this can be observed in the Fig. 1 where the \cancel{E}_T is frequently seen as back-to-back with the leading muon. In order to diminish the contribution of such events, we keep events where : $0.1 rad < \Delta\phi(\mu_1, \cancel{E}_T) < 3 rad$, where $\Delta\phi$ denotes an angular difference in the transverse plan. Due to the limited capacity of PYTHIA to simulate events where the Z is boosted, there is poor agreement between data and MC for low values of the angular difference between μ_1 and μ_2 ; therefore, we keep events where : $1 rad \leq \Delta\phi(\mu_1, \mu_2)$.

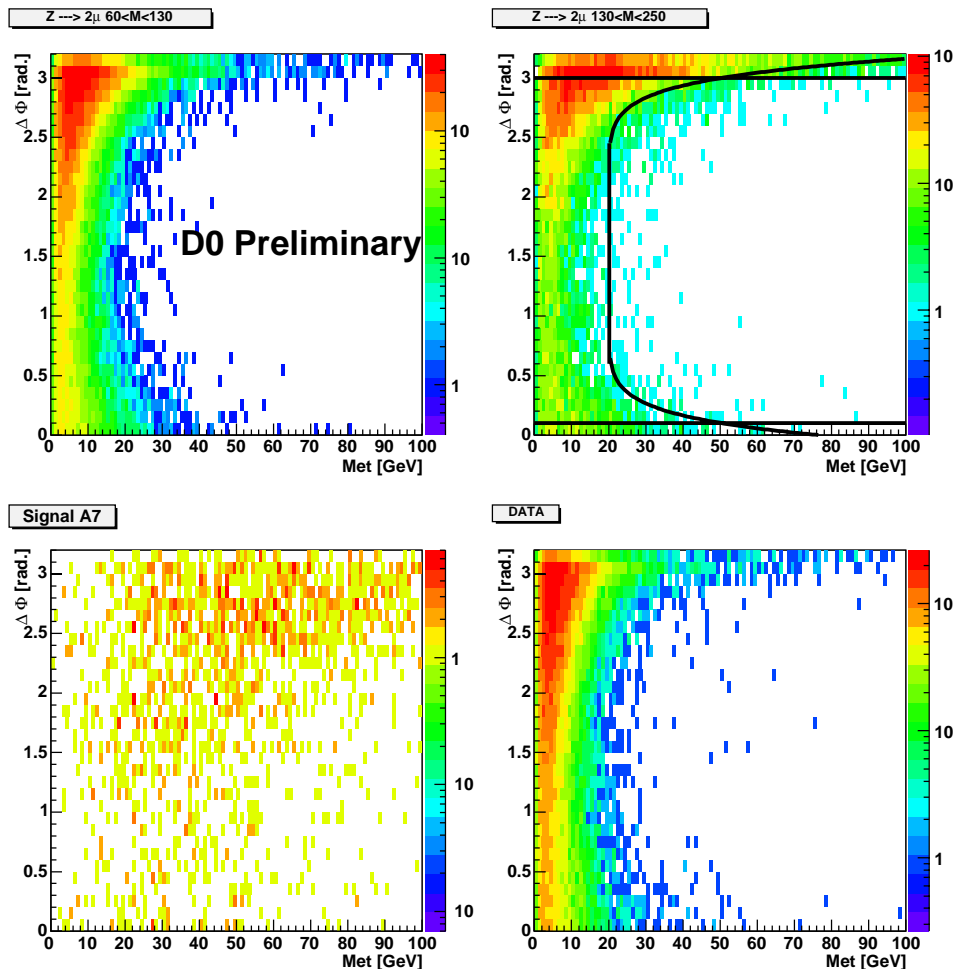


FIG. 1: Angular difference $\Delta\phi(\mu_1, \cancel{E}_T)$ between the leading muon and the \cancel{E}_T versus \cancel{E}_T , after Cut 1 (see Sec. IV), for $Z \rightarrow \mu^+\mu^-$ (top row), signal point A7 and data (bottom row). We require $p_T(\mu_1, \mu_2) > 8, 6$ GeV/c, muon identification, isolation and track quality cuts. The topological cut mentioned in Sec. IV is shown in the top right plot.

The dimuon invariant mass and the muon corrected \cancel{E}_T of the data as well as background and signal contributions are shown in figures 2 and 3 after the muon and $\Delta\phi$ cuts, referred as quality cuts (QC); trigger efficiencies as well as differences of efficiency between data and MC for the different preselection cuts have been taken into account.

Jets are considered in this analysis when fulfilling the conditions :

- matching with a calorimeter object at the level L1 of the trigger,
- $p_T(jet) > 15$ GeV/c,
- $|\eta(jet)| < 2.5$.

The multiplicity of these jets can be seen in the Fig. 4.

IV. SIGNAL SELECTION

As can be seen in the Tab. II, the data is dominated by processes involving the production of the Z boson at the level of quality cuts.

One of the main characteristics of the signal is the presence of jets originating from the hadronization of b quarks. The main background $Z \rightarrow \mu^+\mu^-$ on the other hand, owes the presence of jets to Initial State Radiation gluons which

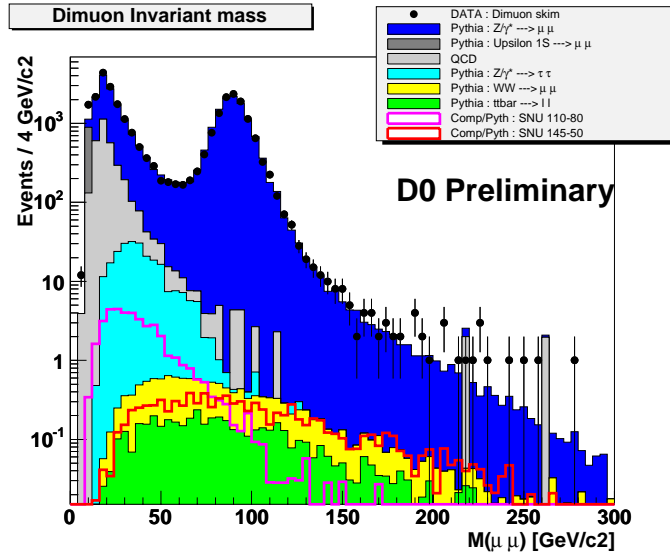
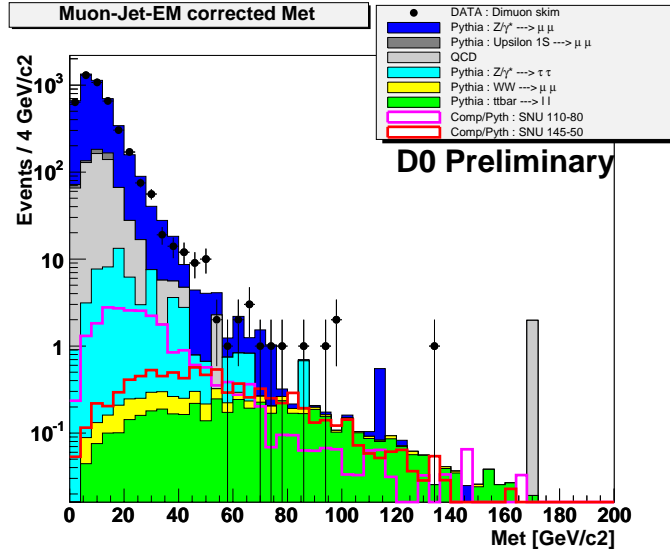


FIG. 2: Dimuon invariant mass after the quality cuts.

FIG. 3: Muon corrected \cancel{E}_T after QC and $N(jet) > 0$ cuts.

hadronize in softer jets, thus resulting in a lower multiplicity of jets; as can be observed in the Fig. 4, the latter is also valid for soft signals which are more limited in phase space. Therefore, in order to keep sensitivity to soft signals while rejecting substantial background, we require :

$$N_{jet} \geq 1 \text{ (Cut 1).}$$

To remove instrumental background from poorly reconstructed muons for the $Z \rightarrow \mu^+ \mu^-$ channel, we require the \cancel{E}_T to be greater than the limit shown on top-right plot of Fig. 1; we will refer to this cut as Cut 2.

Jets originating from the fragmentation of long-living b- or light-quarks have respectively a vertex significantly displaced or close to the primary vertex. Based on the lifetime of hadrons, the Jet Lifetime Probability (JLIP) algorithm calculates the probability for tracks of a jet to originate from the primary interaction point. To further reduce the contribution of the Z background, we consider the JLIP probability of the leading jet ($jet1$) and we require :

$$JLIP(jet1) < 1\% \text{ (Cut 3).}$$

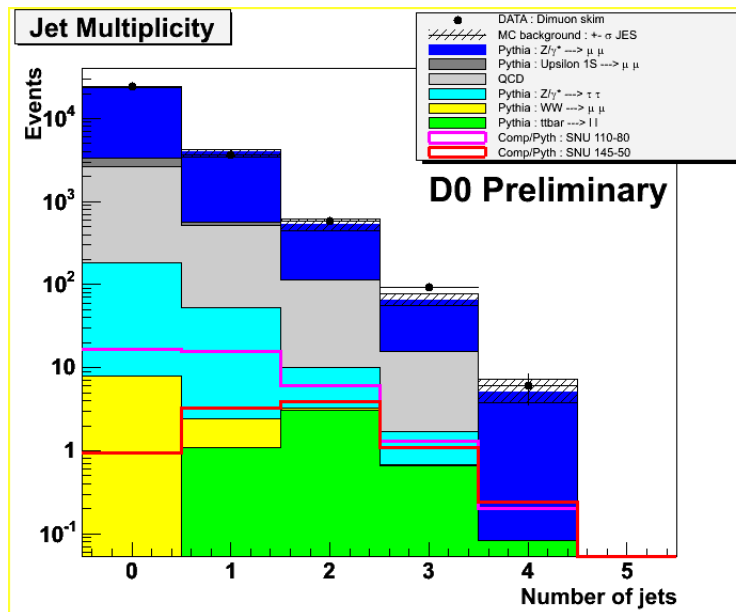


FIG. 4: Multiplicity of jets with $p_T > 15 \text{ GeV}/c$ and $|\eta| < 2.5$ after the quality cuts. The shaded area represents $\pm 1\sigma$ variation of the Jet Energy Scale.

TABLE II: Expected number of events in various background and signal channels, and number of observed events in data, at various levels of the analysis. “QC” refers to the quality cuts mentioned in Sec. III. The two last columns represent the signal points D2 ($M(\tilde{t}_1) = 110 \text{ GeV}/c^2, M(\tilde{\nu}) = 80 \text{ GeV}/c^2$) and A7 ($M(\tilde{t}_1) = 145 \text{ GeV}/c^2, M(\tilde{\nu}) = 50 \text{ GeV}/c^2$). The uncertainties are statistic and JES systematics for the total predicted background and signal events.

Cut	$\Upsilon(1S)$	QCD	$Z \rightarrow \mu^+\mu^-$	$Z \rightarrow \tau^+\tau^-$	WW	$t\bar{t}$	Background	Data	A7	D2
QC	788	3053	23549	233	9.6	5.1	27637 ± 348	28733	9.8	41.1
Cut 1	61	577	3836	59	1.5	5.1	$4539 \pm 97^{+452}_{-553}$	4337	$8.81^{+0.11}_{-0.10}$	$24.14^{+1.46}_{-1.90}$
Cut 2	0	35	136	20	1.1	4.7	$197 \pm 8^{+52}_{-22}$	213	$7.49^{+0.17}_{-0.12}$	$12.92^{+1.21}_{-1.28}$
Cut 3	0	0	5.7	0.44	0.03	2.6	$8.7 \pm 1.6^{+1.3}_{-0.1}$	4	$3.49^{+0.21}_{-0.12}$	$3.37^{+0.37}_{-0.27}$
Cut 4	0	0	0.10	0.44	0.03	2.3	$2.88 \pm 0.43^{+0.10}_{-0.04}$	1	$3.06^{+0.15}$	$3.30^{+0.39}_{-0.27}$

A final anti- Z criterion is to consider the \cancel{E}_T versus the dimuon invariant mass $M(\mu\mu)$. A cut on $M(\mu\mu)$ in the Z peak region only at low \cancel{E}_T is a good solution to further suppress the Z background while preserving the signal points, signal points which are located at higher \cancel{E}_T (compare Fig. 2 and 3) :

$$M(\mu\mu) \notin [75, 120] \text{ GeV}/c^2 \text{ for } \cancel{E}_T < 50 \text{ GeV} \text{ (Cut 4).}$$

The contributions of different backgrounds, expected number of signal events as well as observed data events at different levels of the analysis are summarized in the Tab. II.

V. RESULTS

A. Systematic uncertainties

The main experimental systematic uncertainties are as follows :

- an uncertainty due to the Jet Energy Scale uncertainty [6] between 4% and 22% for high- and low- Δm signal respectively,
- an uncertainty due to b-tagging between null and 10.5% depending on the Δm of the signal,
- an uncertainty due to the muon identification between 2.6% and 7% for low- and high- Δm signal respectively,

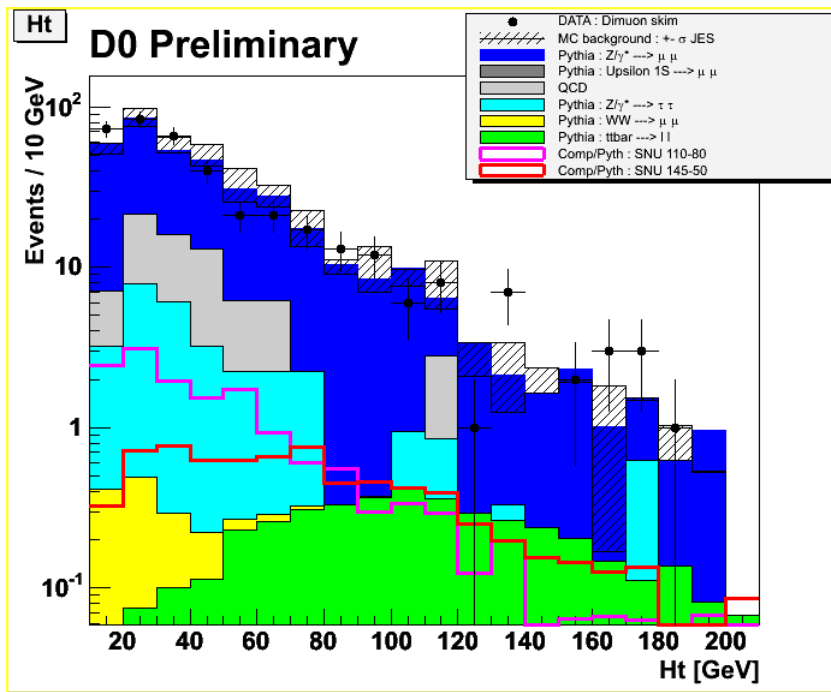


FIG. 5: H_t distribution after quality cuts and $\cancel{E}_T > 20$ GeV. The shaded area represents $\pm 1\sigma$ variation of the Jet Energy Scale.

TABLE III: Expected number of events in remaining background channels after Cut 4 (see Tab. II) and number of observed events in data, for various H_t bins. The first uncertainties are statistic; the systematic uncertainties due to JES, b tagging, muon identification and $t\bar{t}$ cross section uncertainty have been added in quadrature.

H_t bin	Background	Data
[0, 40] GeV	$0.11 \pm 0.02^{+0.02}_{-0.01}$	0
[40, 80] GeV	$0.89 \pm 0.43^{+0.09}_{-0.06}$	0
[80, 120] GeV	$0.75 \pm 0.02^{+0.13}_{-0.09}$	0
[120, 160] GeV	$0.56 \pm 0.02^{+0.07}_{-0.06}$	1
160 GeV <	$0.57 \pm 0.02^{+0.08}_{-0.08}$	0

- a 6.5% uncertainty on the integrated luminosity,
- a 3% uncertainty due to the trigger efficiency,
- the theoretical uncertainty on the $t\bar{t}$ cross section [7].

B. Limits

As can be seen on Tab. II, the $t\bar{t}$ background is the dominating one after the four selection cuts. To reduce this background, we consider the variable H_t defined as the scalar sum of the p_T of all jets passing the identification cuts (see Sec. III) in an event. Fig. 5 shows that the $t\bar{t}$ background dominates at slightly higher values of H_t than the two signal points; furthermore, one can observe that signal points with a low $\Delta m = M(\tilde{t}_1) - M(\tilde{\nu})$ (like the signal point D2) have an H_t distribution centered at lower values than signal points with higher Δm (like signal point A7). Instead of making a requirement on the H_t variable, the H_t spectra predicted for signal and background are compared with the observed H_t spectra when extracting signal limits. The H_t distributions are binned in 40 GeV intervals for this determination. This approach has the advantage of using the full H_t distribution for each point. The expected number of background events in different H_t bins and their corresponding systematic uncertainties as well as observed number of data events are summarized on Tab. III.

After applying the quality (Sec. III) and selection cuts (Sec. IV), the number of data events is in agreement with the expected Standard Model background (see Tab. III). Taking into account the expected number of signal events

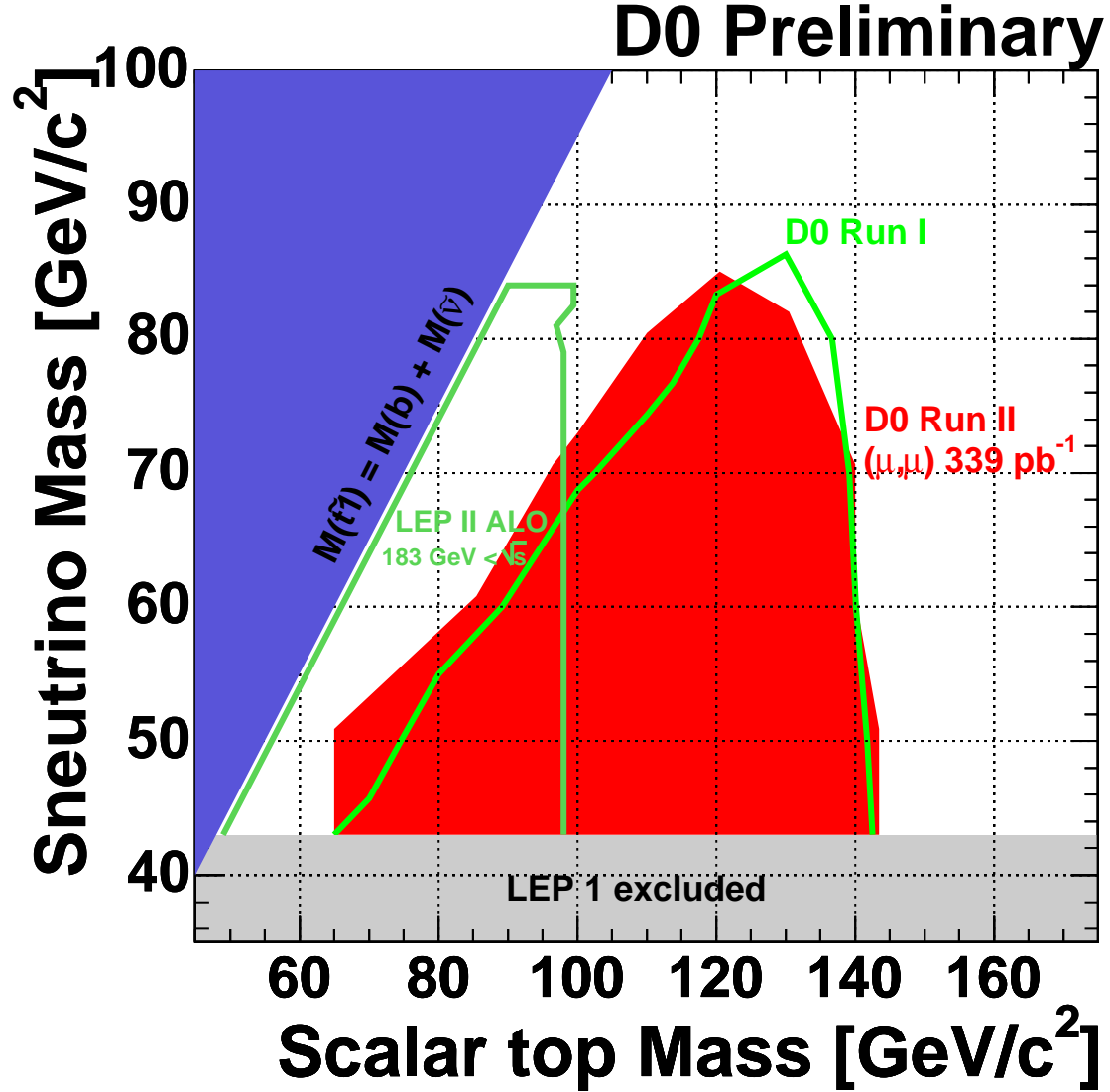


FIG. 6: 95% CL excluded region in the $(M(\tilde{t}_1), M(\tilde{\nu}))$ plan with 339 pb⁻¹ luminosity in the $\mu\mu$ final state. Also shown is the D0 result obtained in Run I with 108 pb⁻¹ luminosity in the $e\mu$ final state.

after all analysis cuts and their corresponding uncertainty, the expected number of background events and the number of observed events in data, we calculate upper-limit cross sections at the 95% Confidence Level (CL) for various signal points; for this purpose a software based on a modified frequentist approach [8] has been used. Regions for which the calculated cross section upper limit is smaller than the theoretical one are 95% CL excluded. Considering the results for different $\tilde{\nu}$ and \tilde{t}_1 mass, we can exclude a region in the $(M(\tilde{t}_1), M(\tilde{\nu}))$ plan as can be seen in the Fig. 6.

Because of the low p_T requirements on the muons, analysis cuts resulting in a low background level, a region in the low Δm phase-space has been excluded which was not excluded in the Run I analysis despite a final state having half the signal branching ratio and fifteen time more non-QCD background.

Acknowledgments

We thank the staffs at Fermilab and collaborating institutions, and acknowledge support from the DOE and NSF (USA); CEA and CNRS/IN2P3 (France); FASI, Rosatom and RFBR (Russia); CAPES, CNPq, FAPERJ, FAPESP and FUNDUNESP (Brazil); DAE and DST (India); Colciencias (Colombia); CONACyT (Mexico); KRF (Korea); CONICET and UBACyT (Argentina); FOM (The Netherlands); PPARC (United Kingdom); MSMT (Czech Republic); CRC Program, CFI, NSERC and WestGrid Project (Canada); BMBF and DFG (Germany); SFI (Ireland); Research Corporation, Alexander von Humboldt Foundation, and the Marie Curie Program.

-
- [1] H. P. Nilles, Phys. Rep. 32, 249 (1977).
 - [2] C. Boehm, A. Djouadi, Y. Mambrini, “Decays of the lightest top squark”, Physical Review D. Volume 61, 095006.
 - [3] A. Pukhov et al., “CompHEP- a package for evaluation of Feynman diagrams and integration over multi-particle phase space”, User’s manual for version 3.3, Preprint INP-MSU 98-41/542.
 - [4] T. Sjostrand, Comp. Phys. Comm 82, 74, (1994).
 - [5] W. Beenakker, R. Hoepker, M. Spira, “PROSPINO, a program for the PROduction of Supersymmetric Particles In Next-to-leading Order QCD”, hep-ph/9611232.
 - [6] V.M. Abazov et al., “Measurement of Dijet Azimuthal Decorrelations at Central Rapidities in $p\bar{p}$ Collisions at $\sqrt{s} = 1.96$ TeV”, hep-ex/0409040.
 - [7] N. Kidonakis and R. Vogt, Phys. Rev. **D 68** (2003) 114014.
 - [8] “Search for the Standard Model Higgs Boson at LEP”, hep-ex/0107029.